NUMERICAL SIMULATION OF UNDEREXPANDED CRYOGENIC HYDROGEN JETS

Zhang, Y.P.[1], Nie, S.S.[2], Liu, H.[3], Yu, A.F.[4], Yao, C.Y.[5], Ba, Q.X.[6], Xiao, J.S.[7] and Li, X.F.[8,*]
[1] Institute of Thermal Science and Technology (Institute for Advanced Technology), Shandong University, Jingshi Road, Jinan, 250061, China, zhangyp7613@163.com
[2] Institute of Thermal Science and Technology (Institute for Advanced Technology), Shandong University, Jingshi Road, Jinan, 250061, China, niesshuai@outlook.com
[3] Sinopec Research Institute of Safety Engineering Co.,Ltd., Songling Road, Qingdao, 266000, China, liuh.qday@sinopec.com
[4] Sinopec Research Institute of Safety Engineering Co.,Ltd., Songling Road, Qingdao, 266000, China, yuaf.qday@sinopec.com
[5] Institute of Thermal Science and Technology (Institute for Advanced Technology), Shandong University, Jingshi Road, Jinan, 250061, China, yaochenyi0417@163.com
[6] School of Mechanical Engineering, Shandong University, Jingshi Road, Jinan, 250061, China, qingxin90113@126.com
[7] Hubei Research Center for New Energy & Intelligent Connected Vehicle, School of Automotive Engineering, Wuhan University of Technology, Luoshi Road, Wuhan, 430070, China, Jinsheng.Xiao@uqtr.ca
[8] Institute of Thermal Science and Technology (Institute for Advanced Technology), Shandong University, Jingshi Road, Jinan, 250061, China, lixf@email.sdu.edu.cn

ABSTRACT

As a clean and renewable energy carrier, hydrogen is one of the most promising alternative fuels. Cryogenic compressed hydrogen can achieve high storage density without liquefying hydrogen, which has good application prospects. Investigation of the safety problems of cryogenic compressed hydrogen is necessary before massive commercialization. The present study modeled the instantaneous flow field using the Large Eddy Simulation (LES) for cryogenic (50 and 100 K) underexpanded hydrogen jets released from a round nozzle of 1.5 mm diameter at pressures of 0.5-5.0 MPa. The simulation results were compared with the experimental data for validation. The axial and radial concentration and velocity distributions were normalized to show the self-similar characteristics of underexpanded cryogenic jets. The shock structures near the nozzle were quantified to correlate the shock structure sizes to the source pressure and nozzle diameter. The present study on the concentration and velocity distributions of underexpanded cryogenic hydrogen jets is useful for developing safety codes and standards.

Keywords: cryogenic hydrogen; hydrogen safety; underexpanded jets; self-similarity

1.0 INTRODUCTION

Large-scale implementation of renewable energy sources is crucial for addressing the challenges posed by the depletion of fossil fuel reserves, geopolitical tensions, and environmental pollution. Hydrogen is a highly accessible energy carrier with a high calorific value and zero carbon emissions when used as a fuel. Currently, over 30 governments have pledged to incorporate hydrogen as a clean energy vector into their energy systems. Hydrogen and its derivatives are expected to play a critical role in the decarbonization of sectors that face challenges in reducing emissions, such as heavy industry, shipping, aviation and heavy-duty transport, where alternative solutions are either unavailable or difficult to implement [1].

At present, the storage and transportation technology of high-pressure gaseous hydrogen is relatively well developed, with the primary ways being high-pressure vessels and long-tube trailer transportation. High-pressure gaseous hydrogen storage and transportation have the advantages of

well-established technology, low energy consumption, and fast hydrogen filling. However, the density of room-temperature compressed hydrogen is not high enough for massive, long-distance transportation. Although liquid hydrogen has a high density, the technology for hydrogen liquefaction is not yet well developed, and the liquefaction consumes a significant amount of energy. Cryogenic compressed hydrogen can achieve much higher density than room-temperature compressed hydrogen and does not need to liquefy the hydrogen. The tank materials and fatigue strength of materials of cryogenic compressed hydrogen tanks have been analyzed to verify the feasibility of cryogenic compressed hydrogen storage for vehicle use [2].

Hydrogen is the smallest molecule among all elements, which makes it more prone to leakage or permeation from high-pressure environments. Cryogenic compressed hydrogen leakage can form an underexpanded hydrogen jet when the pressure ratio across the nozzle is above the critical pressure ratio. The minimum ignition energy, ignition limit range, and energy density of hydrogen indicate that hydrogen can be ignited easily and will release a large amount of thermal energy [3]. Therefore, it is essential to study the characteristics of underexpanded cryogenic hydrogen jets to achieve the large-scale application of cryogenic compressed hydrogen storage.

Several release experiments have been performed to study the cryogenic and room-temperature under-expanded hydrogen jets. Sandia National Laboratories has conducted experiments to create an underexpanded hydrogen jet with a 10:1 pressure ratio (stagnation to ambient pressure) from a 0.75 mm nozzle and atmospheric free jet [4]. Laboratory measurements were made on the concentration and temperature fields of cryogenic hydrogen jets for nozzle pressures ranging from 0.2 to 0.5 MPa and nozzle temperatures ranging from 50 to 61 K [5]. They found that the average centerline mass fraction was observed to decay at a rate similar to room-temperature hydrogen jets, while the half-width of the Gaussian profiles of the mass fraction was observed to spread more slowly than for room-temperature hydrogen. Kobayashi et al. [6-7] measured the concentrations and temperature of hydrogen flowing through 0.2-0.7 mm diameter nozzles from 55 to 281.5 K at pressures of 14.8-90.0 MPa. The axial hydrogen concentration distribution obtained by the ambient temperature (300 K) hydrogen injection test well agreed with the experimental formula based on previous research studies. Li et al. [8] measured underexpanded, cryogenic hydrogen and methane jets using laser Raman scattering diagnostic. The time-averaged concentration and temperature data were analyzed. The results showed that the centerline RMS mass fraction decays similarly to the mean mass fraction.

Many studies have used various turbulent models to simulate underexpanded cryogenic hydrogen jets. Ba et al. [9] modeled cryogenic hydrogen releases using the LES turbulence model for a 1 mm diameter round nozzle for reservoir pressures of 0.2-1.0 MPa. The concentration, temperature and velocity fields were predicted and normalized to analyze the self-similar characteristics. Ren et al. [10] analyzed the detailed nearfield flow structures and transient physics of the underexpanded cryogenic hydrogen jets using high-resolution direct numerical simulations (DNS). The influences of the nozzle pressure ratio and exit diameter on the nearfield jet dynamics were studied. Giannissi et al. [11] used the k-ε model to simulate hydrogen releases with reservoir pressure from 0.2 to 0.5 MPa and reservoir temperature from 50 and 58 K. The predicted centerline mass fraction agreed well with that of the experiment data of 0.3 MPa release, but for the test with 0.3 and 0.4 MPa release, the concentration was overpredicted.

The accuracy of CFD model predictions is limited by the turbulence model. LES turbulent model resolves large eddies directly and models small eddies. The fluctuation characteristics of the jet parameters can be obtained with LES. This paper used the LES model to simulate the underexpanded cryogenic hydrogen jets in 6 scenarios. The time-averaged and fluctuation characteristics of the calculated concentration and velocity data were analyzed.

2.0 NUMERICAL MODELS

2.1 Governing Equations

Three-dimensional compressible Navier–Stokes equations are solved to model the underexpanded jet with the LES turbulence model including the energy equation and the species transport equation. In LES, large eddies are resolved directly, while small eddies are modeled. LES, therefore, falls between DNS and RANS in terms of the fraction of the resolved scales. The real gas density was calculated by the Soave-Redlich-Kwong real gas equation of state. The species equations can be written as

$$\frac{\partial}{\partial t}(\rho Y_i) + \nabla(\rho \vec{v} Y_i) = -\nabla \cdot \vec{J}_i + R_i + S_i \tag{1}$$

where Y_i is the local mass fraction of each species. $\vec{J}_i$ is the diffusion flux of species i. In turbulent flows, Fluent computes the mass diffusion in the following form:

$$\vec{J}_i = -\left(\rho D_{i,m} + \frac{\mu_t}{Sc_t}\right)\nabla Y_i - D_{T,i}\frac{\nabla T}{T} \tag{2}$$

where Sc_t is the turbulent Schmidt number. $D_{T,i}$ is the turbulent diffusivity.

The LES governing equations can be written as

$$\frac{\partial \rho}{\partial t} + \frac{\partial}{\partial x_i}(\rho \overline{u}_i) = 0 \tag{3}$$

$$\frac{\partial}{\partial x_i}(\rho \overline{u}_i) + \frac{\partial}{\partial x_j}(\rho \overline{u}_i \overline{u}_j) = \frac{\partial}{\partial x_j}(\sigma_{ij}) - \frac{\partial \overline{p}}{\partial x_i} - \frac{\partial \tau_{ij}}{\partial x_j} \tag{4}$$

The stress tensor σ_{ij} is defined by

$$\sigma_{ij} = \left[\mu\left(\frac{\partial \overline{u}_i}{\partial x_j} + \frac{\partial \overline{u}_j}{\partial x_i}\right)\right] - \frac{2}{3}\mu\frac{\partial \overline{u}_l}{\partial x_l}\delta_{ij} \tag{5}$$

The subgrid-scale (SGS) stresses τ_{ij} resulting from the filtering operation are unknown, and require modeling. The subgrid-scale turbulence models employ the Boussinesq hypothesis as in the RANS models, computing subgrid-scale turbulent stresses from

$$\tau_{ij} = \frac{1}{3}\tau_{kk}\delta_{ij} - 2\mu_t \overline{S}_{ij} \tag{6}$$

The subgrid-scale kinetic energy is defined as

$$k_{sgs} = \frac{1}{2}\left(\overline{u_k^2} - \overline{u}_k^2\right) \tag{7}$$

The subgrid-scale turbulent viscosity μ_t is computed using k_{sgs} as

$$u_t = C_k \rho k_{sgs}^{1/2} \Delta_f \tag{8}$$

2.2 Numerical Conditions

As shown in Fig. 1, the cryogenic compressed hydrogen stored in a tank releases through a 1.5 mm diameter round nozzle into a three-dimensional cylindrical computational domain. The length of the cylindrical computational domain is 240 mm and the diameter is 120 mm. The grid around the nozzle outlet is refined and smoothed to ensure calculation accuracy. The ambient air temperature is 300 K and the ambient pressure is 0.101 MPa. Six scenarios were simulated as shown in Table 1.

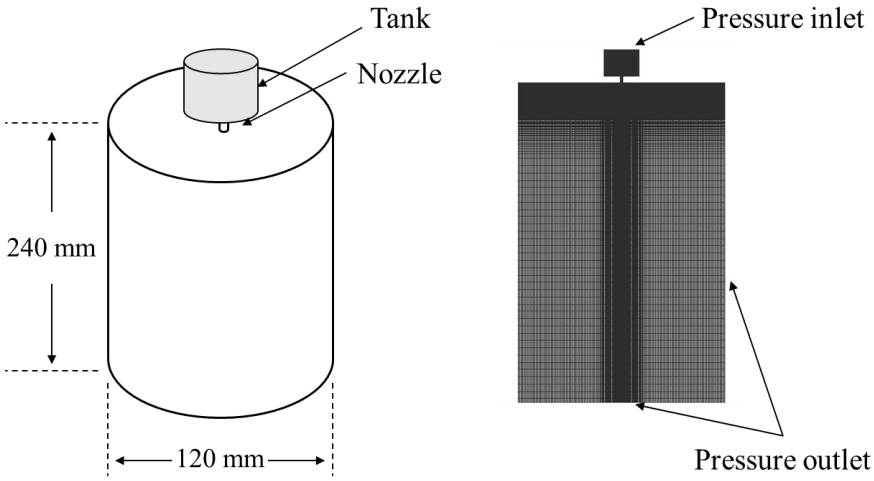

Figure 1. The computational domain and the grid

Table 1. Summary of inflow parameters.

Scenarios	Inlet pressure (MPa)	Inlet temperature (K)
Case 1	0.5	50
Case 2	0.8	50
Case 3	1.0	50
Case 4	1.0	100
Case 5	2.0	50
Case 6	5.0	50

2.3 Modeling Validation and Grid Sensitivity Analysis

The hydrogen jet centerline mole fractions were compared with the experimental data for a 0.3 MPa, 51 K release from a 1.25 mm diameter nozzle [5]. As shown in Fig. 2, the calculated results are in good agreement with the experiment results.

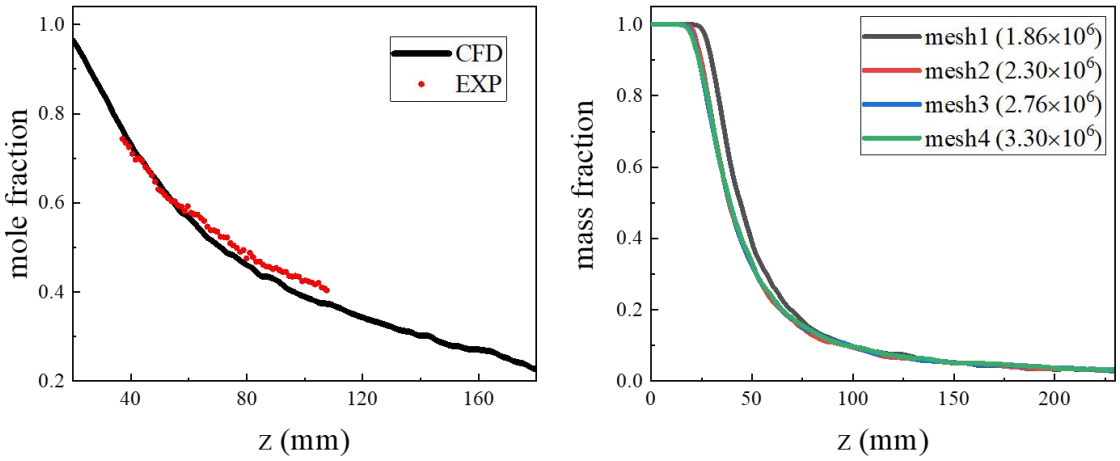

Figure 2. Modeling validation (left) and grid sensitivity analysis results (right)

Four grids were set up for grid sensitivity analysis. Mesh 1 contains 1860000 elements, mesh 2 contains 2300000 elements, mesh 3 contains 2760000 elements, and, mesh 4 contains 3300000 elements. The calculated jet centerline hydrogen mass fractions for a 1 MPa, 75 K release from a nozzle with a 1.5 mm diameter are shown in Fig. 2. The distance z from the nozzle is expressed in millimeters. The calculated results with mesh 2, mesh 3, and mesh 4 are similar. There is no significant effect of continuing to increase the number of grids on the calculation results. This study used 2760000 elements to reduce the calculation time and ensure calculation accuracy.

3.0 RESULTS AND DISCUSSION

3.1 Concentration Distributions

The normalized distance ζ is defined as $\zeta = z/d^*$, $d^* = d\sqrt{\rho_0/\rho_a}$, where d is the nozzle diameter, ρ_0 is the stagnation density at the nozzle outlet and ρ_a is the ambient air density. The inverse time-averaged mass fraction at the centerline $\overline{Y}_{cl}$ decays linearly with the normalized distance ζ, as shown in Fig. 3. The correlation between inverse time-averaged mass fraction and normalized distance can be written as

$$\frac{1}{\overline{Y}_{\mathrm{cl}}} = C_1 \frac{z}{d^*} \tag{9}$$

where C_1 is the centerline mass fractions decay rate. The correlation between inverse time-averaged mass fraction and normalized distance has been observed for a range of jet releases. The axis mass fractions decay rate has been measured to be 0.21~0.271 [12-13]. The C_1 obtained from the simulations in this paper is 0.248, which is in the above range. The calculated axis mass fractions decay rate of cryogenic hydrogen jets is similar to that of room-temperature jets.

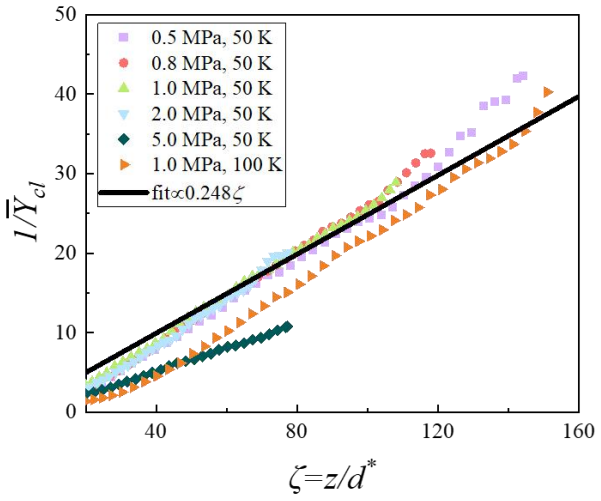

Figure 3. The centerline mass fraction decays

Fig. 4 shows the calculated data points at several downstream distances, along with a fit of a Gaussian curve for the normalized hydrogen mass fraction as a function of the normalized radius for the given release conditions in the upper-left corner of each subplot. $\overline{Y}$ is the time-averaged hydrogen mass fractions in the radial direction at a given location. r is the radial coordinate.

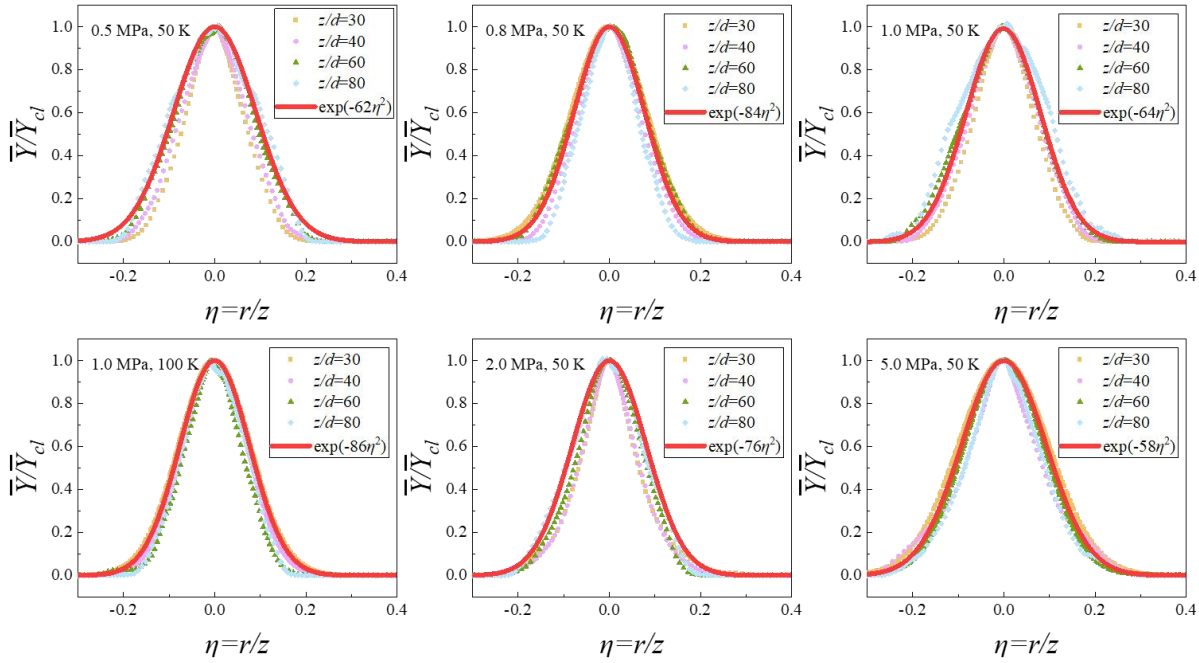

Figure 4. Normalized radial mass fractions ($\eta = r/z$)

The red line in each plot is the Gaussian fit for the simulation conditions. The Gaussian fit line of 5.0 MPa, 50 K is the widest with a fit of $\overline{Y}/\overline{Y}_{\rm cl} = \exp(-58\eta^2)$. The Gaussian fit line of 1.0 MPa, 100 K is the narrowest with a fit of $\overline{Y}/\overline{Y}_{\rm cl} = \exp(-86\eta^2)$. The fit for room-temperature jets to the normalized radial mass fractions is $\overline{Y}/\overline{Y}_{\rm cl} = \exp(-59\eta^2)$ [4,12-13], which is slightly wider than the simulated underexpanded cryogenic hydrogen jets.

The release of cryogenic compressed hydrogen through a nozzle can form an underexpanded jet, which is highly turbulent. The study of the turbulence properties of underexpanded jets is useful for

solving related hydrogen safety problems. This paper investigates the fluctuation characteristics of the hydrogen jet concentration. The centerline unmixedness [4,15], which is defined as the ratio of RMS to mean mass fraction $Y'/\overline{Y}_{cl}$, is characterized by the normalized distance z/d as shown in Fig. 5, where Y' is the RMS mass fractions, $\overline{Y}_{cl}$ is the time-averaged mass fractions.

The unmixedness of simulated data is centered about an asymptotic value of 0.243 which is near the range of 0.21-0.24 [13-16]. The centerline RMS mass fraction decay rate is 0.243 and the mean mass fraction decay rate is 0.248. The centerline RMS mass fraction decays similarly to the mean mass fraction. The results show that the concentration fluctuations of the underexpanded cryogenic hydrogen jet can be accurately predicted with the LES model.

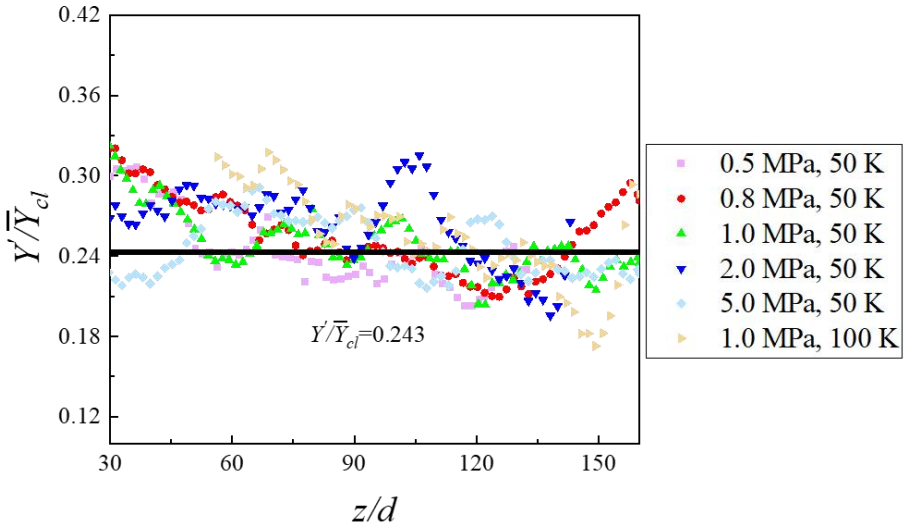

Figure 5. The centerline unmixedness of hydrogen jets

3.2 Velocity Distributions

This paper simulated the underexpanded cryogenic hydrogen jet velocity distributions for 6 conditions with the LES model. The first normal shock called Mach disk appears near the nozzle outlet as P_0/P_∞ (the nozzle pressure ratio, NPR) increases, where P_0 is the stagnation pressure, P_∞ is the ambient pressure. The simulated Mach disk in various conditions is shown in Fig. 6. The area above 3 MPa is shown in white in Fig. 6. The horizontal position of the Mach disk is marked by dotted lines.

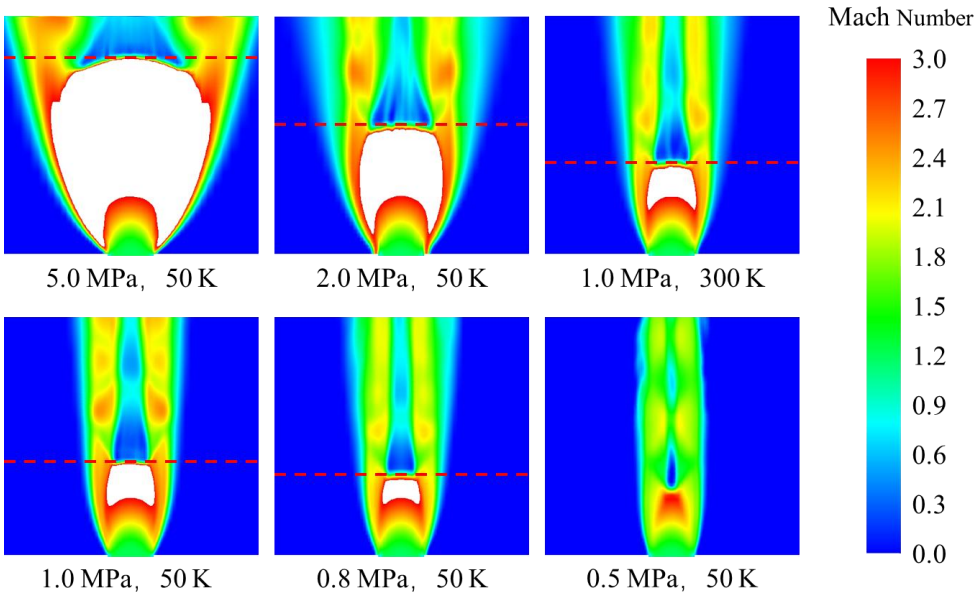

Figure 6. Mach number in various simulation conditions

The distance between the Mach disk and nozzle outlet increases as the NPR increases. The correlation between the distance from the Mach disk and nozzle outlet and NPR can be written as [17-18]

$$\frac{Z_m}{d} = C_2 (P_0/P_\infty)^{0.5} \tag{10}$$

where Z_m the distance between the Mach disk and nozzle outlet, d is the nozzle outlet diameter and C_2 is the proportionality coefficient.

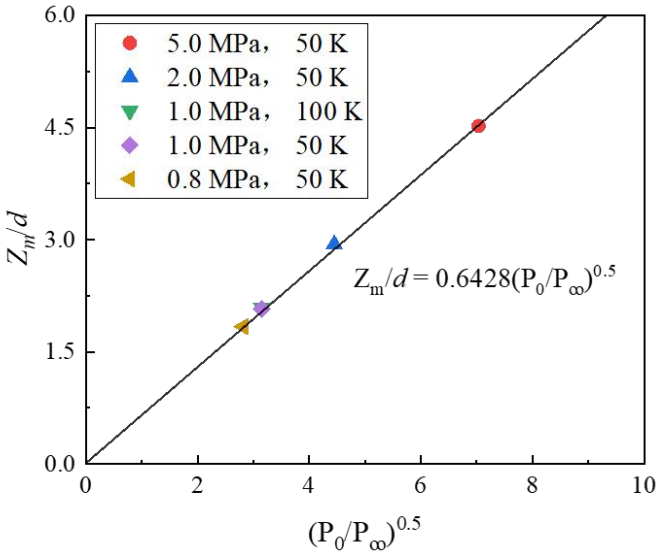

Figure 7. Correlation of simulated Mach disk location and NPR

The correlation of simulated Mach disk location and NPR is shown in Fig. 7. The slope C_2 was obtained by fitting equal to 0.6428. The proportionality coefficient for room temperature is in the range of 0.65-0.67, which is slightly more than 0.6428. The results show that the Mach disk location of 5 MPa, 50 K release is 0.05-0.19 mm less than that of the room temperature.

The normalized inverse time-averaged velocity $u_0/\overline{u}_{cl}$ at the centerline decays linearly with the normalized distance ζ, as shown in Fig. 8. The correlation between the normalized inverse time-averaged velocity and normalized distance can be written as

$$u_0/\overline{u}_{\mathrm{cl}} = C_3 \frac{z}{d^*} \tag{11}$$

where C_3 is the centerline velocity decay rate, u_0 is the nozzle outlet velocity. C_3 for simulated data is 0.148, which is near the velocity decay rate of 0.16 [19-20] for room-temperature releases. The calculated results show that the centerline velocity decay of underexpanded cryogenic hydrogen jets is similar to that of room-temperature underexpanded hydrogen jets.

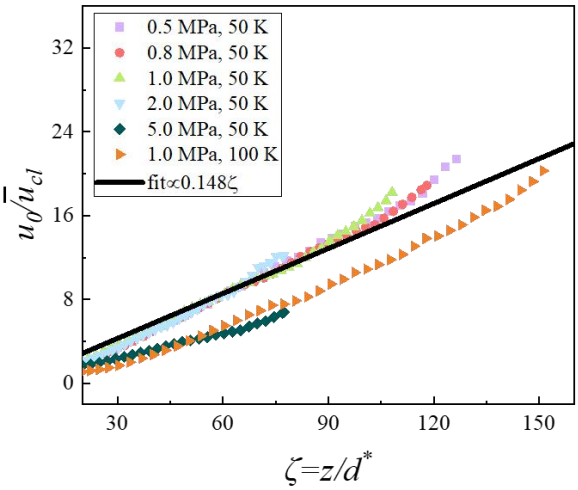

Figure 8. The centerline velocity decays

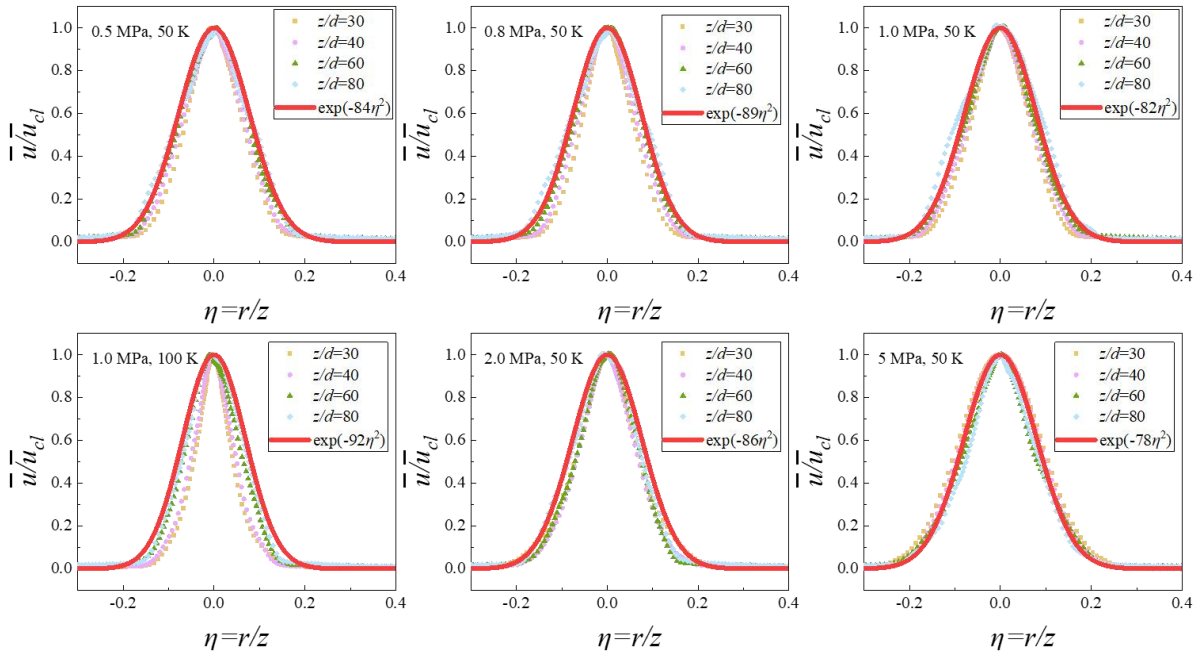

Figure 9. Normalized radial velocity ($\eta = r/z$)

Fig. 9 shows the calculated data points at several downstream distances, along with a fit of a Gaussian curve for the normalized hydrogen velocity as a function of the normalized radius for the given release

conditions in the upper-left corner of each subplot. $\overline{u}$ is the time-averaged hydrogen velocity in the radial direction at a given location. r is the radial coordinate.

The red line in each plot is the Gaussian fit for the simulation conditions. The Gaussian fit line of 5.0 MPa, 50 K is the widest with a fit of $\overline{Y}/\overline{Y}_{\mathrm{cl}} = \exp(-78\eta^2)$. The Gaussian fit line of 1.0 MPa, 100 K is the narrowest with a fit of $\overline{Y}/\overline{Y}_{\mathrm{cl}} = \exp(-92\eta^2)$. The fit for room-temperature jets to the normalized radial mass fractions is $\overline{Y}/\overline{Y}_{\mathrm{cl}} = \exp(-75.2\eta^2)$ [15], which is near to the simulated underexpanded cryogenic hydrogen jets.

The corresponding profiles of velocity (RMS) fluctuations along the centerline, $u'/\overline{u}_{\mathrm{cl}}$ and $v'/\overline{u}_{\mathrm{cl}}$, are shown in Fig. 10 and Fig. 11. The axial RMS velocity u' and radial RMS velocity v' along the centerline are normalized by the mean centerline velocity $\overline{u}_{\mathrm{cl}}$. The simulation results show that the axial RMS velocity fluctuations are higher than the radial component. The black line ($u'/\overline{u}_{\mathrm{cl}} = 0.28$) in Fig. 10 is measured for an air jet into ambient air [21], which is slightly greater than the calculated data. The radial velocity fluctuations measured in a small-scale unintended release of hydrogen experiment asymptote to a value of about 0.23 [12]. The calculated radial velocity fluctuations for $z/d > 90$ fit well as $v'/\overline{u}_{\mathrm{cl}} = 0.23$ shown in Fig. 11. The results show that the velocity fluctuations of the underexpanded cryogenic hydrogen jets can be accurately predicted with the LES model.

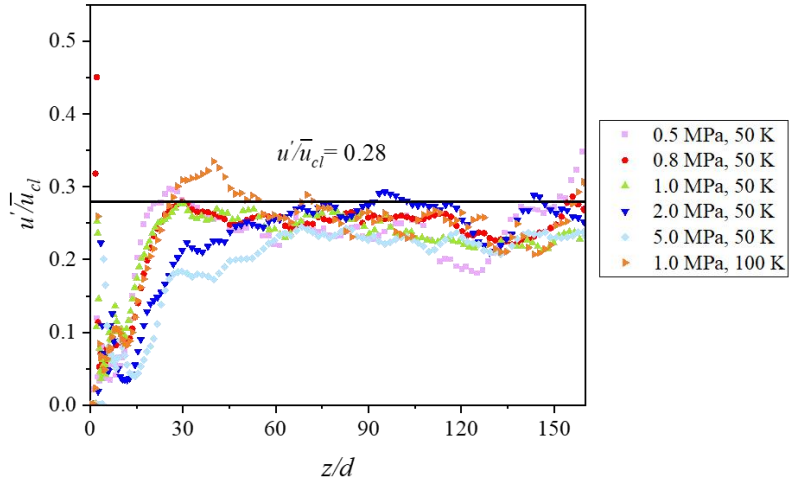

Figure 10. Axial velocity fluctuations along the centerline

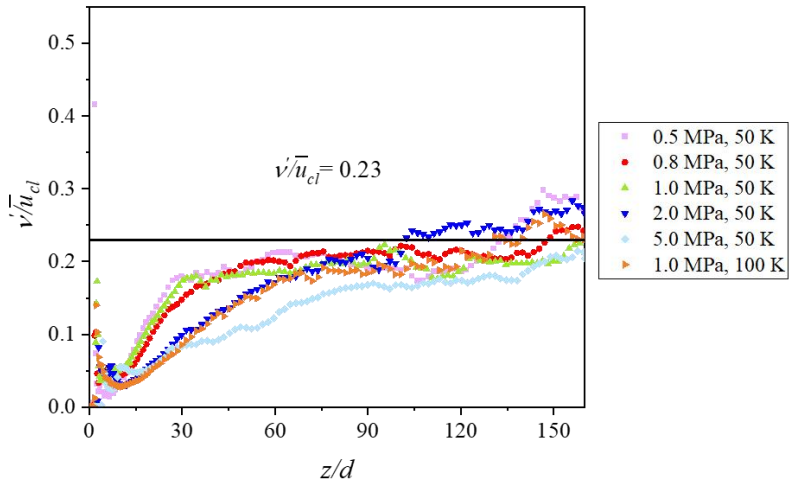

Figure 11. Radial velocity fluctuations along the centerline

4.0 CONCLUSIONS

The present study modeled the instantaneous flow field using the Large Eddy Simulation (LES) for cryogenic (50 and 100 K) underexpanded hydrogen jets released from round nozzles of 1.5 mm at pressures of 0.5-5 MPa. Three-dimensional compressible Navier–Stokes equations are solved to model the underexpanded jets with the LES turbulence model. The concentration and velocity distribution of underexpanded cryogenic hydrogen jets were calculated.

The simulation results of time-averaged concentration and velocity were plotted to show a hyperbolic decay law along the jet centerline and a Gaussian distribution in the radial direction. The predicted centerline decay rate for the normalized mass fraction is 0.248, which is in the range of 0.21-0.271 for room-temperature releases. The radial distribution of the normalized concentration was slightly narrower than that of the room temperature. The predicted centerline decay rate for the normalized velocity is 0.148, which is slightly less than the decay rate for temperature releases of 0.16. The Gaussian distribution of the simulated normalized radial velocity is similar to that of room-temperature jets. The Mach disk location of various numerical conditions was modeled with the correlation formula written as $Z_m/d = 0.6428\,(P_0/P_\infty)^{0.5}$. The slope of 0.6428 is near the predicted locations for room-temperature jets.

The centerline concentration and velocity fluctuation characteristics of underexpanded cryogenic hydrogen jets have been studied. The simulated concentration fluctuation (unmixedness) is centered about an asymptotic value of 0.243, which is similar to that of the room-temperature jets. The centerline RMS mass fraction decays similarly to the mean mass fraction. The axial and radial velocity fluctuations calculated along the centerline have been normalized by the time-averaged centerline velocity. The results show similarity to the room temperature experimental data.

The present study on the concentration and velocity distributions of underexpanded cryogenic hydrogen jets is essential to developing safety codes and standards.

REFERENCE

1. IEA, Hydrogen, Paris: IEA, 2022. https://www.iea.org/reports/hydrogen.
2. Brunner, T. and Kircher, O., Cryo-Compressed Hydrogen Storage, Hydrogen Science and Engineering: Materials, Processes, Systems and Technology, 2016, pp. 711–732.
3. Yang, F.Y., Wang, T.Z., Deng, X.T., Dang, J., Huang, Z.Y., Hu, S., Li, Y.Y. and Ouyang, M.G., Review on hydrogen safety issues: Incident statistics, hydrogen diffusion, and detonation process, *International Journal of Hydrogen Energy*, **46**, 61,2021, pp. 31467-31488.
4. Ruggles, A.J., Statistically advanced, self-similar, radial probability density functions of atmospheric and under-expanded hydrogen jets, *Exp Fluids*, **56**, 202, 2015.
5. Hecht, E.S. and Panda, P.P., Mixing and warming of cryogenic hydrogen releases, *International Journal of Hydrogen Energy*, **44**, 17, 2019, pp. 8960-8970.
6. Kobayashi, H., Naruo, Y., Maru, Y., Takesaki, Y. and Miyanabe, K., Experiment of cryo-compressed (90-MPa) hydrogen leakage diffusion, *International Journal of Hydrogen Energy*, **43**, 37, 2018, pp. 17928-17937.
7. Kobayashi, H., Daimon, Y., Umemura, Y., Muto, D., Naruo, Y. and Miyanabe, K., Temperature measurement and flow visualization of cryo-compressed hydrogen released into the atmosphere, *International Journal of Hydrogen Energy*, **43**, 37, 2018, pp. 17938-17953.
8. Li, X.F., Yao, C.Y., Egbert, S.C., He, Q., Zhao, Z.Y., Christopher, D.M. and Hecht, E.S., Self-similar characteristics of underexpanded, cryogenic hydrogen and methane jets, *International Journal of Hydrogen Energy*, **48**, 10, 2023, pp. 4104-4117.

9. Ba, Q.X., He, Q., Zhou, B., Chen, M.J., Li, X.F. and Cheng, L., Modeling of cryogenic hydrogen releases, *International Journal of Hydrogen Energy*, **45**, 55, 2020, pp. 31315-31326.
10. Ren Z., Wen J.X., Numerical characterization of under-expanded cryogenic hydrogen gas jets, *AIP Advances*, **10**, 2020.
11. Giannissi, S.G., Venetsanos, A.G. and Hecht, E.S., Numerical predictions of cryogenic hydrogen vertical jets, *International Journal of Hydrogen Energy*, **46**, 23, 2021, pp.12566-12576.
12. Schefer, R.W., Houf, W.G. and Williams, T.C., Investigation of small-scale unintended releases of hydrogen: Buoyancy effects, *International Journal of Hydrogen Energy*, **33**, 17, 2008, pp. 4702-4712.
13. Richards, C.D. and Pitts, W.M., Global density effects on the self-preservation behavior of turbulent free jets, *Journal of Fluid Mechanics*, **254**, 1993, pp. 417-435.
14. Panchapakesan, N.R. and Lumley, J.L., Turbulence measurements in axisymmetric jets of air and helium. Part 1. Air jet, *Journal of Fluid Mechanics*, **246**, 1993, 197-223.
15. Ruggles, A.J. and Ekoto, I.W., Ignitability and mixing of underexpanded hydrogen jets, *International Journal of Hydrogen Energy*, 37, 22, 2012, pp. 17549-17560.
16. Panchapakesan, N.R. and Lumley, J.L., Turbulence measurements in axisymmetric jets of air and helium. Part 2. Helium jet, *Journal of Fluid Mechanics*, **246**, 1993, 197-223.
17. Ashkenas H., The Structure and Utilization of Supersonic Free Jets in Low Density Wind Tunnels., *Rarefied Gas Dynamics*, 1966.
18. Davidor, W. and Penner S.S., Shock standoff distances and Mach-disk diameters in underexpanded sonic jets, *AIAA J*, **9**, 8, 1971, pp. 1651-1653.
19. Yüceil, K.B., and Ötügen, M.V., Scaling parameters for underexpanded supersonic jets. *Physics of Fluids*, **14**, 2002, pp. 4206-4215.
20. Zaman K. B. M. Q., Asymptotic spreading rate of initially compressible jets—experiment and analysis, *Physics of Fluids*, **10**, 1998, 2652.
21. Wygnanski, I. and Fiedler, H.E., Some measurements in the self-preserving jet, *Journal of Fluid Mechanics*, **38**, 3, 1969, pp. 577-612.